2012

Kerama Gap 2009-2011 Data Report

Zhaojun Liu

Hanna Na

Hirohiko Nakamura

Ayako Nishina

Jae-Hun Park

See next page for additional authors

Graduate School of Oceanography
University of Rhode Island
Narragansett, Rhode Island 02882-1197

Kerama Gap
2009-2011
Data Report

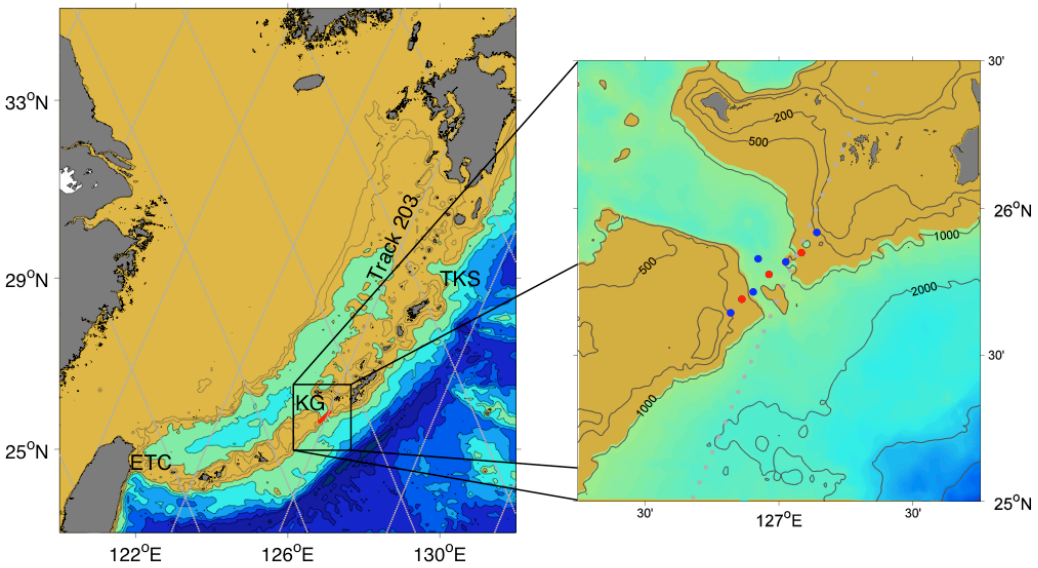

Zhaojun Liu[2]
Hanna Na[1]
Hirohiko Nakamura[2]
Ayako Nishina[2]
Jae-Hun Park[1,3]
Karen Tracey[1]
Mark Wimbush[1]

[1]Graduate School of Oceanography, University of Rhode Island, Narragansett, RI 02882-1197, U.S.A.
[2]Faculty of Fisheries, Kagoshima University, 4-50-20, Shimoarata, Kagoshima, 890-0056, Japan
[3]Korea Institute of Ocean Science and Technology, 787, Haeanro, Ansan 426-744, Korea

GSO Technical Report No. 2012-02

Table of Contents

List of Figures

List of Tables

1. Introduction

The principal flows in and out of the East China Sea (ECS) are through channels penetrating the Ryukyu Ridge between Taiwan and Kyushu (Figure 1.1). Since ~20 Sv of Kuroshio mean flow enters and exits through two of these channels, they are especially well known: the East Taiwan Channel (sill depth 775 m) at the ridge's southwestern end, and the Tokara Strait (sill depth 690 m) near its northeastern end [*Choi et al.,* 2002]. But the *deepest* channel connecting the ECS to the surrounding ocean is near the ridge mid-point: it is the Kerama Gap (KG), about 50 km wide with sill depth 1050 m [*Choi et al.,* 2002]—see Figure 1.1.

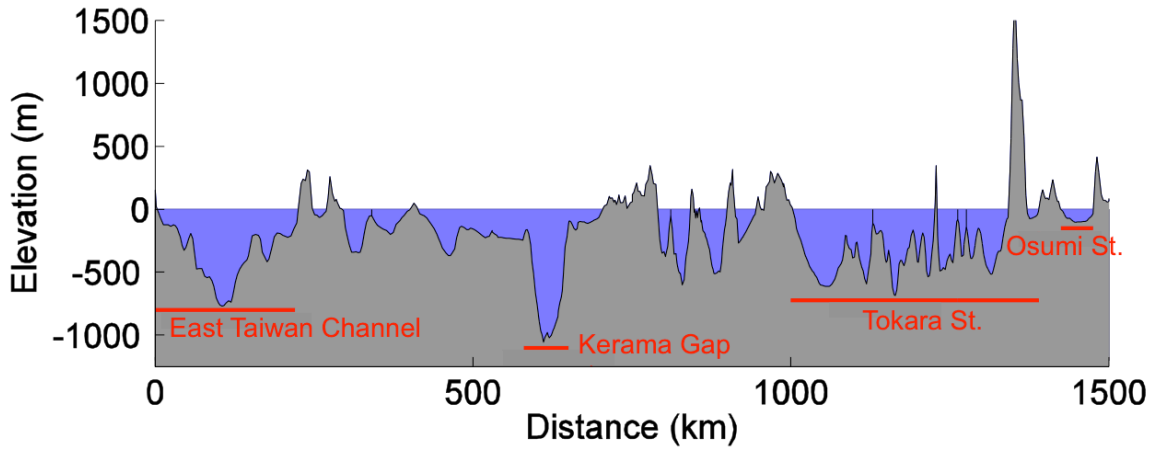

Figure 1.1 The Ryukyu ridgeline, from Taiwan (on the left) to Kyushu, Japan (on the right). The island of Okinawa is at Distance = 700-800 km, just to the right (i.e., northeast) of the Kerama Gap.

The University of Rhode Island (URI), in the USA, and Kagoshima University (KU), in Japan, jointly undertook a study of the time variability of flow through the Kerama Gap. To accomplish this, an array of Current-and-Pressure-sensor-equipped Inverted Echo Sounder (CPIES) and Current Meter (CM) moorings was deployed in the KG during June 2009 and maintained until June 2011. The CPIES and CM moorings were intended to provide data enabling us to determine the upper-layer (depth<500 m) and lower-layer (depth>500m) flows, respectively.

2. Mooring Measurements

2.1 *CPIES*

The CPIES is a recording multi-sensor instrument which is deployed on the seafloor. It combines an Inverted Echo Sounder (IES) measuring round-trip acoustic travel time (τ) from the seafloor to the sea surface, with a precision pressure (P) and temperature (T) Digiquartz sensor (see Table 2.3.1 for Model numbers) and an Aanderaa (Model 3820R)

current-velocity ($\vec{U}$) sensor positioned 50 m above. As programmed, the CPIES instruments emitted, every hour, six sets of four 12-kHz acoustic pings at 10-minute intervals; ping echo times from the sea surface were measured. The pressure sensor in each instrument measured hourly near-bottom pressure and temperature during a 16 s interval following the first burst of four acoustic pings. In addition, the current sensor measured the components of horizontal current (as well as temperature) about 50 m above the seafloor. For a full description of the CPIES instruments used, see the following webpage:

http://www.po.gso.uri.edu/dynamics/IES/index.html

On each of three cruises (June 2009, 2010, 2011), hydrographic data were acquired with a CTD (SeaBird Model 911 plus); on the two later cruises, velocity data were obtained with a shipboard ADCP (RDI Ocean surveyor 75 kHz). Since the shipboard ADCP was out of order during the 2009 cruise, two LADCPs (RDI WorkHorse 300 kHz) were attached to the CTD frame, one aimed upward and one downward, to obtain velocity profiles, but because of a data recovery problem, no useful LADCP data were obtained.

2.2 *CM*

A point measurement current meter, 3-D Acoustic Current Meter (3D-ACM) (Falmouth Scientific, Inc.), was used on all current-meter moorings. A standard 3D-ACM with optional pressure sensor records N/S, E/W, and U/D (Up/Down) velocity components, temperature, and pressure. The method of velocity measurement is briefly described as follows: The 3D-ACM has 4 acoustic-path axes, each comprising a pair of transducer-receiver pair. Only 3 axes not significantly contaminated by the wake from the central support strut are required for a complete solution of *X*, *Y* and *Z* components of velocity. Magnetic direction from a 3 axis magnetometer and tilt from 2 electrolytic tilt sensors are processed with *X*, *Y* and *Z* components of velocity in the microprocessor to determine N/S, E/W and U/D (Up/Down) components for vector averaging. These averages were taken over 5 minutes once and hour. Nominal specifications of the 3D-ACM measurement are given in Table 2.2.1.

Table 2.2.1. 3D-ACM specifications.

Parameter	Type	Range	Accuracy	Resolution
Velocity	Acoustic (phase shift)	0–300 cm/s	± 1.0 cm/s	0.1 cm/s
Direction	3 axis fixed fluxgate	0–360 deg.	± 1.0 deg	0.1 deg.
Tilt	2 axis electrolytic	0–25 deg.	± 0.2 deg.	0.01 deg.
Temperature	Thermistor	-2–35 °C	± 0.05 °C	0.005 °C
Pressure	Strain	3400 db	± 0.5% F.S.	0.1 db

2.3 *Mooring Locations*

Locations of the CPIES and CM moorings are listed in Tables 2.3.1 and 2.3.2, respectively. These locations are shown in Figure 2.3.1 on a map of the region. Figure 2.3.2 shows instrument positions on a cross-section of the Kerama Gap at the main mooring array.

Table 2.3.1. CPIES mooring locations and depths. "Bottom depth" is depth recorded by the ship's fathometer. "Mean pressure" is mean pressure recorded by the CPIES. Note: the current sensor in each case was 50m above the sea bed (under low-current conditions). "Spacing" is distance between neighboring CPIES moorings along the main mooring array. "Year 1" is June 2009– June 2010; "Year 2" is June 2010– June 2011. Pressure sensors with Model numbers 46K and 410K have respectively 6,000 psi and 10,000 psi ratings.

CPIES mooring	Year	Latitude (°N)	Longitude (°E)	Spacing (km)	Bottom depth (m)	Mean pressure (dbar)	CPIES serial no.	Pressure sensor Model/ serial no.	Current sensor serial no.
ES1	1&2	25.6436	126.8203	11.58	564	588	231	46K/109333	502
ES2	1	25.7155	126.9040		1081	1107	045	46K/109331	312
	2	25.7155	126.9040	16.46	1081	1101	063	46K/109321	n/a
ES3	1	25.8167	127.0248		1029	1061	036	46K/109330	308
	2	25.8157	127.0244	16.23	1032	1038	140	410K/91877	755
ES4	1&2	25.9173	127.1418		506	532	053	46K/109324	306
ES5	1	25.8287	126.9234		1416	1476	063	46K/109321	310

Table 2.3.2. CM mooring locations and depths, including individual current-meter depths. "Year 1" is June 2009– June 2010; "Year 2" is June 2010– June 2011. "Spacing" is distance between neighboring CM moorings.

CM mooring	Year	Latitude (°N)	Longitude (°E)	Spacing (km)	Bottom depth (m)	Measurement depth (m)	Sensor serial no.
CM1	1	25.691	126.862		783	443	1641
						698	1632
	2	25.692	126.864		783	443	1640
						698	1574
CM2	1	25.770	126.970	13.95	1160	365	1644
						620	1634
						975	1576
	2	25.780	126.964		1199	548	1642
						753	1633
						1008	1591
CM3	1	25.865	127.075	14.52	810	470	1646
						725	1554
	2	25.849	127.085		808	468	1643
						723	1573

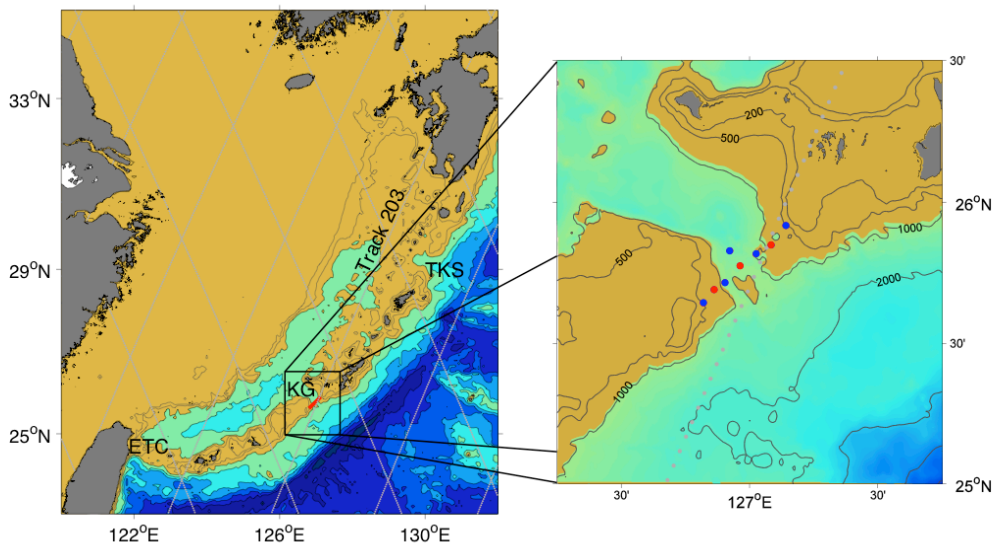

Figure 2.3.1. Left panel: East China Sea (ECS) region; ETC = East Taiwan Channel, KG = Kerama Gap, TKS = Tokara Strait; Jason-1 altimetry tracks shown as gray lines; red bar shows position of the deployed array. Right panel: Enlargement of Kerama Gap region showing the deployed array: blue dots are CPIES moorings, red dots are CM moorings. The array is along a line across the Kerama Gap (see Fig. 3), except that one CPIES instrument near the center of the Gap is about 7.4 km northwest of this line. Depth contours are at 200, 500, 1000, 2000, 3000 and 4000 m; dotted gray line is the Jason-1 altimetry track.

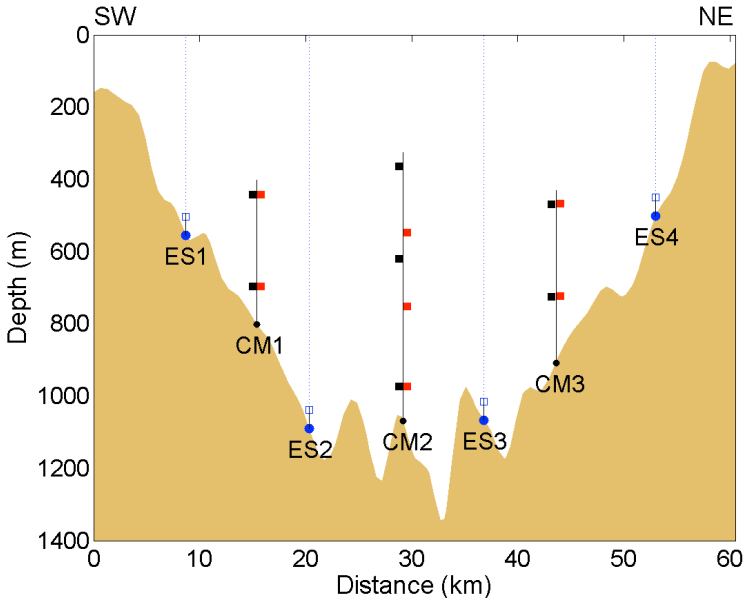

Figure 2.3.2. Cross-section diagram of the main Kerama Gap array. Four CPIESs are shown as solid blue dots (open blue squares immediately above represent the current sensors 50 m above the seafloor). Seven CMs on three moorings are shown as solid black (Year 1) and red (Year 2) squares. Topography is from measurements taken on the June 2009 cruise. Note: this section across the Kerama Gap is slightly northwest of the sill, hence the maximum depth at the section is greater than the sill depth (1050 m).

2.4 *Data*

All the current meters on the CM moorings provided excellent quality data throughout the two-year study. Moreover the data records are complete, except that the shallowest current meter (365-m depth on CM2) was severed from the central CM mooring, 2010 February 9; a Japanese fisherman found it, together with its floatation, drifting on the surface near the Tokara Strait. Thanks to this fisherman, good Year-1 data from the current meter were recovered up to the time of severance.

Data recovery from our CPIES moorings was less successful. CPIESs from the deep (~1,000 m depth) region of the KG all suffered leaks from apparent fish-bites on the 50-m electrical cables connecting the current-sensors to the main instruments. As a result, data from these CPIES instruments are fragmentary. Fortunately, the two shallowest (~500 m depth) CPIESs (ES1 and ES4) were undamaged and obtained good data throughout the two-year deployment period.

3. Mooring Data Processing

3.1 *CM*

3.1.1 Pressure (*P*) and Temperature (*T*)

In order to determine the depth of each CM, the shallowest CM on each CM mooring included a pressure sensor. All pressure records from these CMs were averaged for the whole observational period, and then converted to depth in meters using the hydrostatic equation assuming that 1025 kg m^{-3} density and 9.8 m s^{-2} gravity. Other CM depths were calculated by adding cable lengths to the depth of the CM with pressure sensor. The results are summarized in Tables 2.3.2 and 3.1.2.1.

Temperature records were lowpass filtered using a 2nd order Butterworth filter, run forward and backward, with cutoff period of 50 hours. Daily mean values were calculated from ensemble averages for each day. The results are shown in Figures 3.1.1.1 and 3.1.1.2.

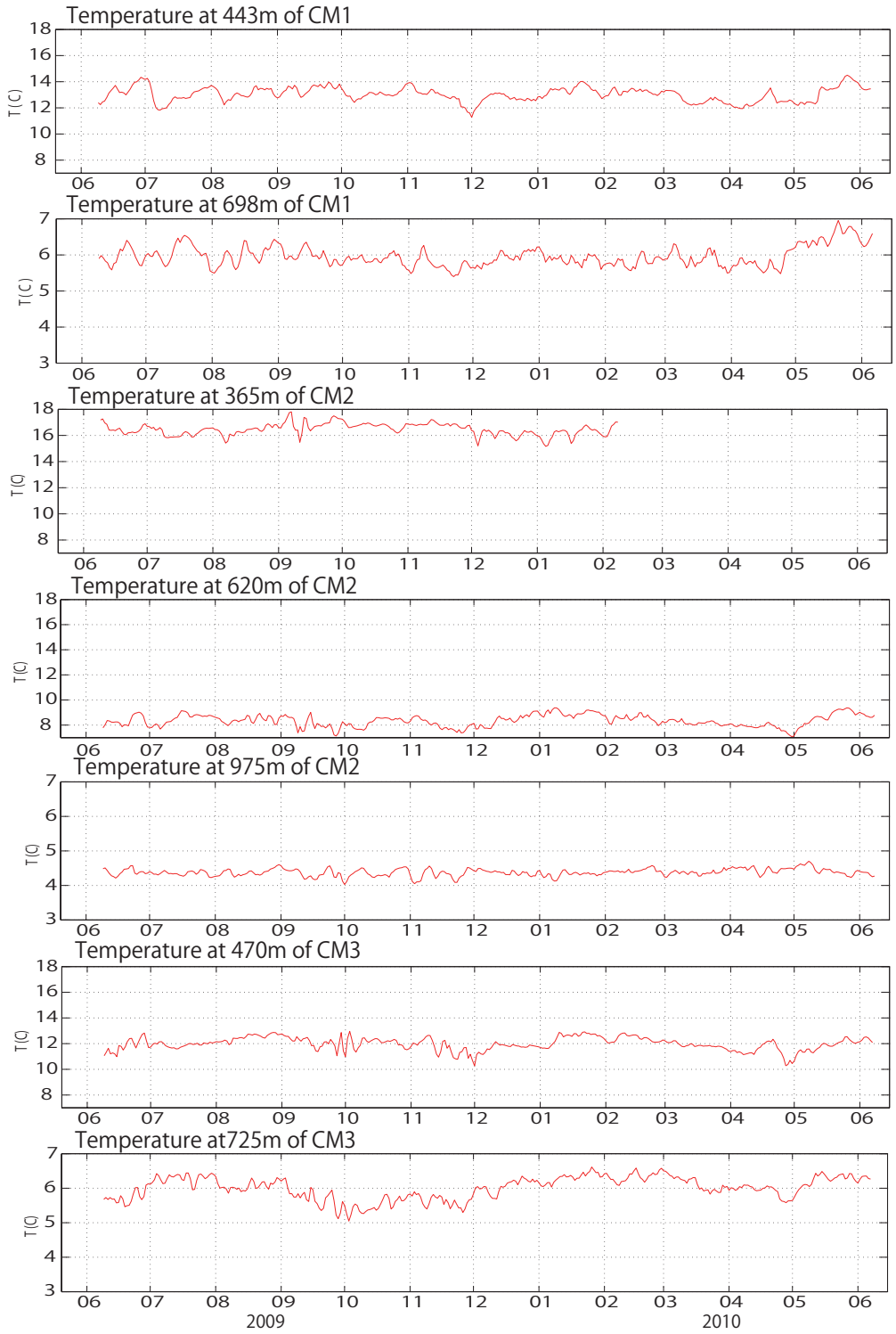

Figure 3.1.1.1. Time series of 3D-ACM temperature for Year 1 (June 2009 – June 2010).

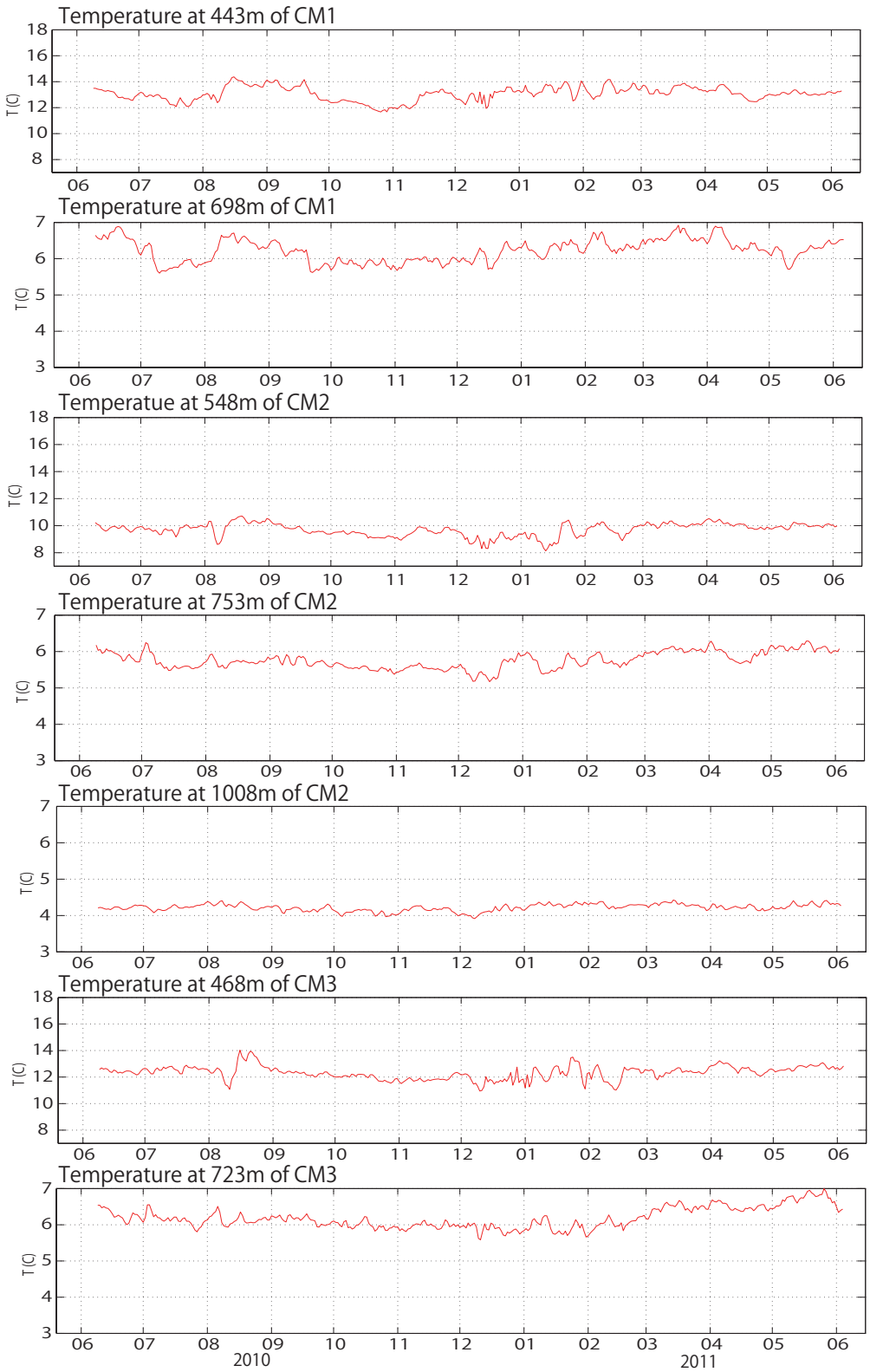

Figure 3.1.1.2. Time series of 3D-ACM temperature for Year 2 (June 2010 – June 2011).

3.1.2 Velocity

Current records at all CM moorings were corrected (using a routine from NOAA's National Geophysical Data Center, see http://www.ngdc.noaa.gov/geomagmodels/) for the local magnetic declination at each time and at each site (see Table 3.2.1.1 for mean values), so *U* is true eastward and *V* is true northward. The velocities were then lowpass filtered using a 2nd order Butterworth filter, run forward and backward, with cutoff period of 50 hours. Daily mean values were calculated from ensemble averages for each day. The results are shown in Figures 3.1.2.1 to 3.1.2.6. Table 3.1.2.1 gives basic statistics for the currents at all CM moorings.

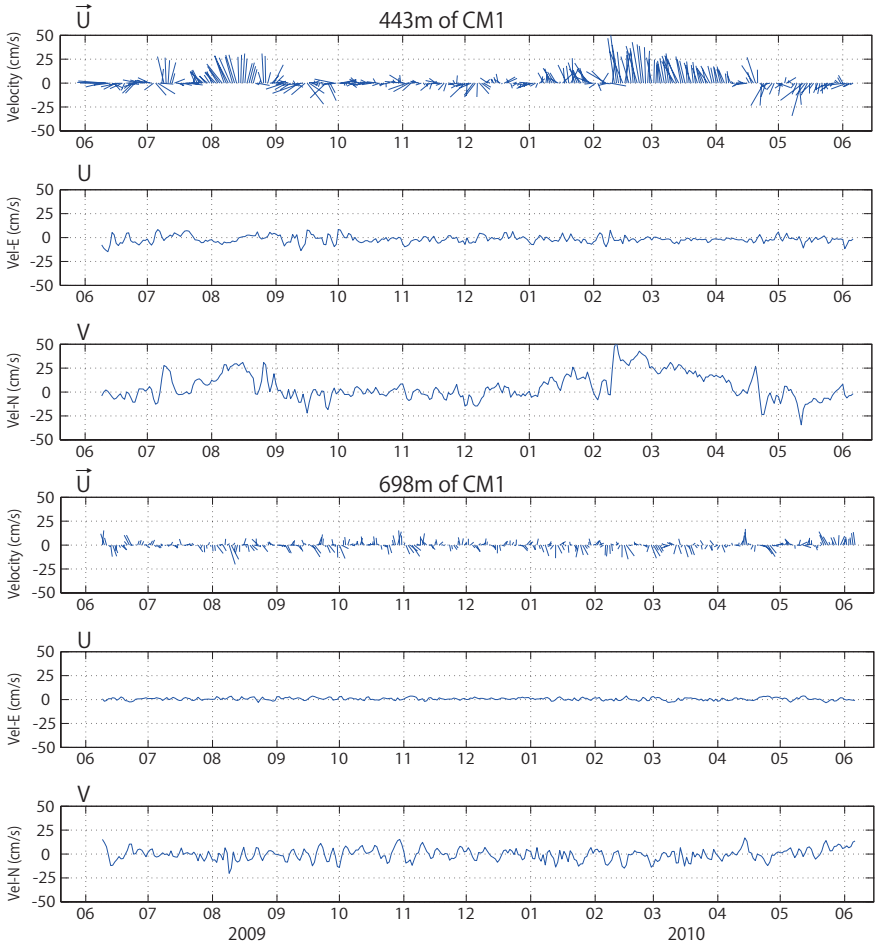

Figure 3.1.2.1. Time series of 3D-ACM current velocities at CM1 for Year 1 (June 2009 – June 2010).

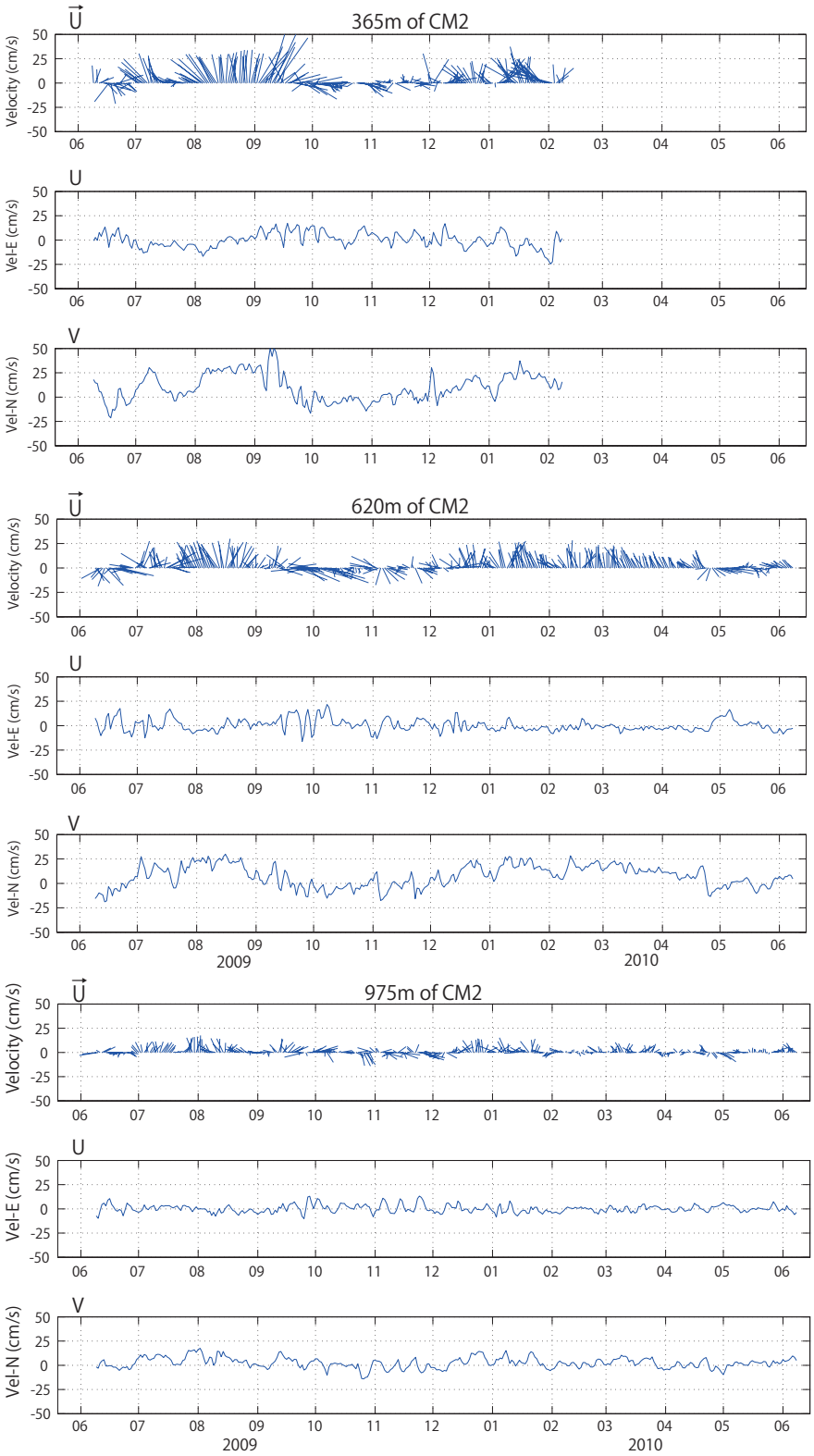

Figure 3.1.2.2. Time series of 3D-ACM current velocities at CM2 for Year 1 (June 2009 – June 2010).

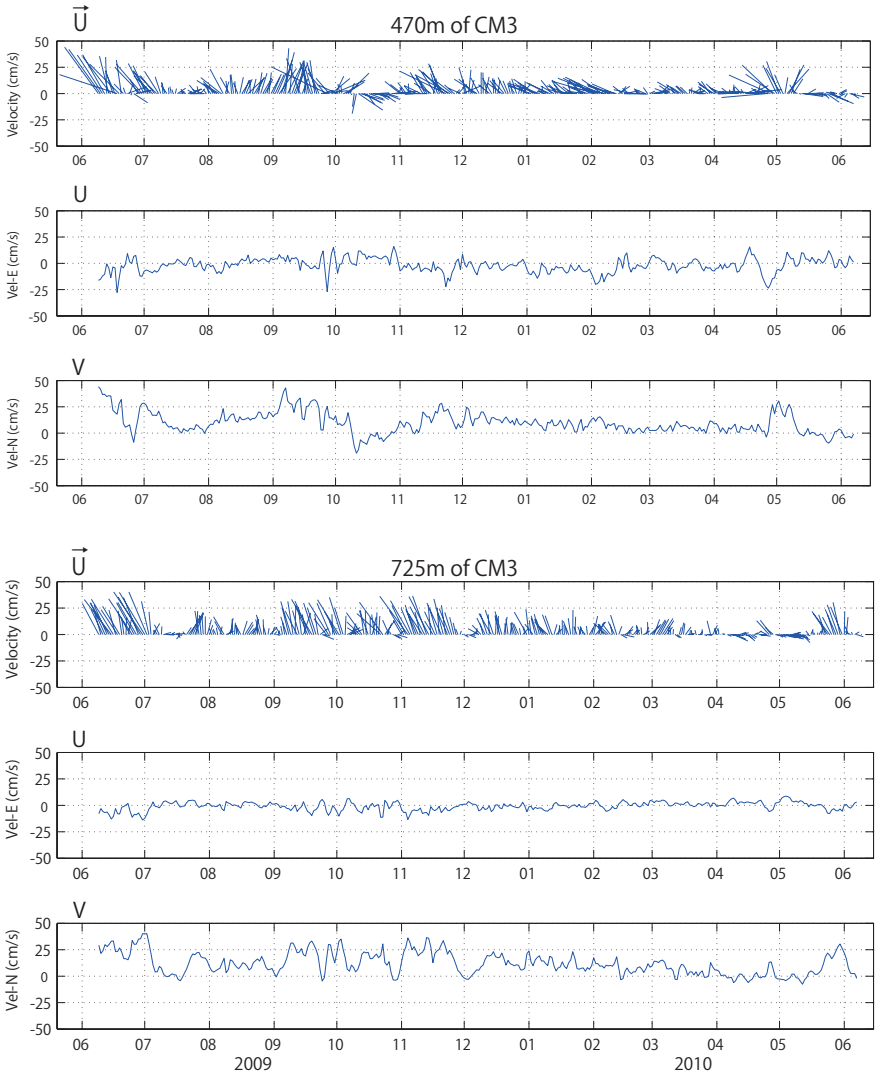

Figure 3.1.2.3. Time series of 3D-ACM current velocities at CM3 for Year 1 (June 2009 – June 2010).

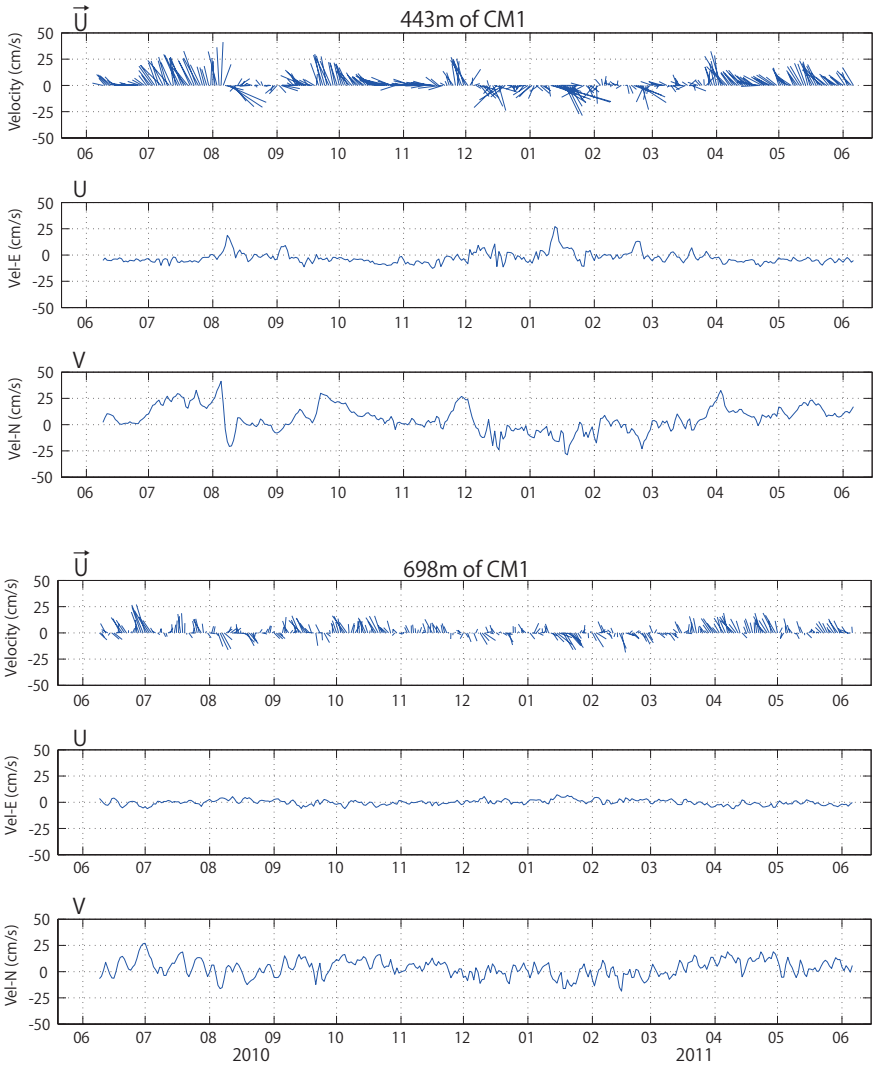

Figure 3.1.2.4. Time series of 3D-ACM current velocities at CM1 for Year 2 (June 2010 – June 2011).

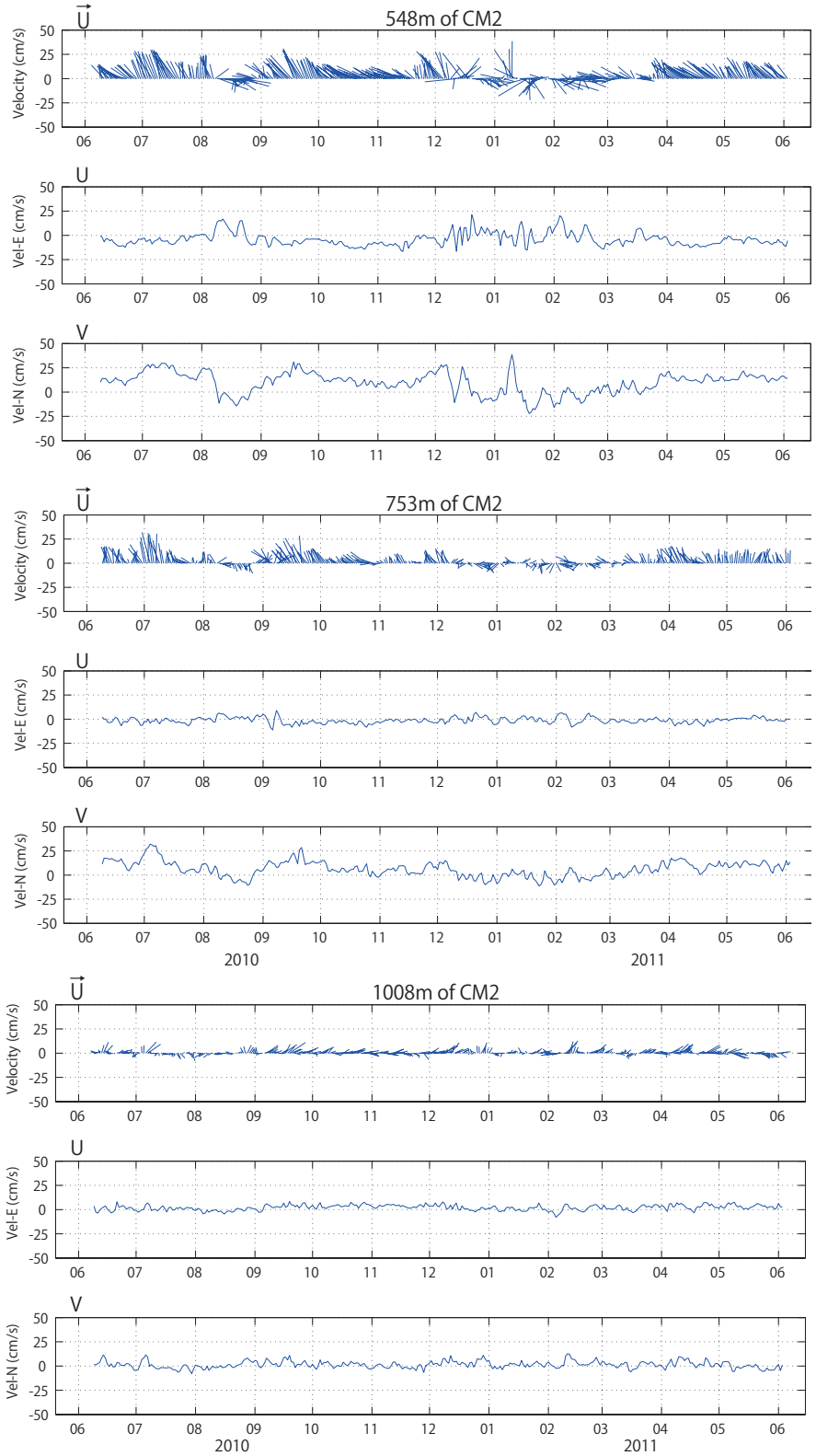

Figure 3.1.2.5. Time series of 3D-ACM current velocities at CM2 for Year 2 (June 2010 – June 2011).

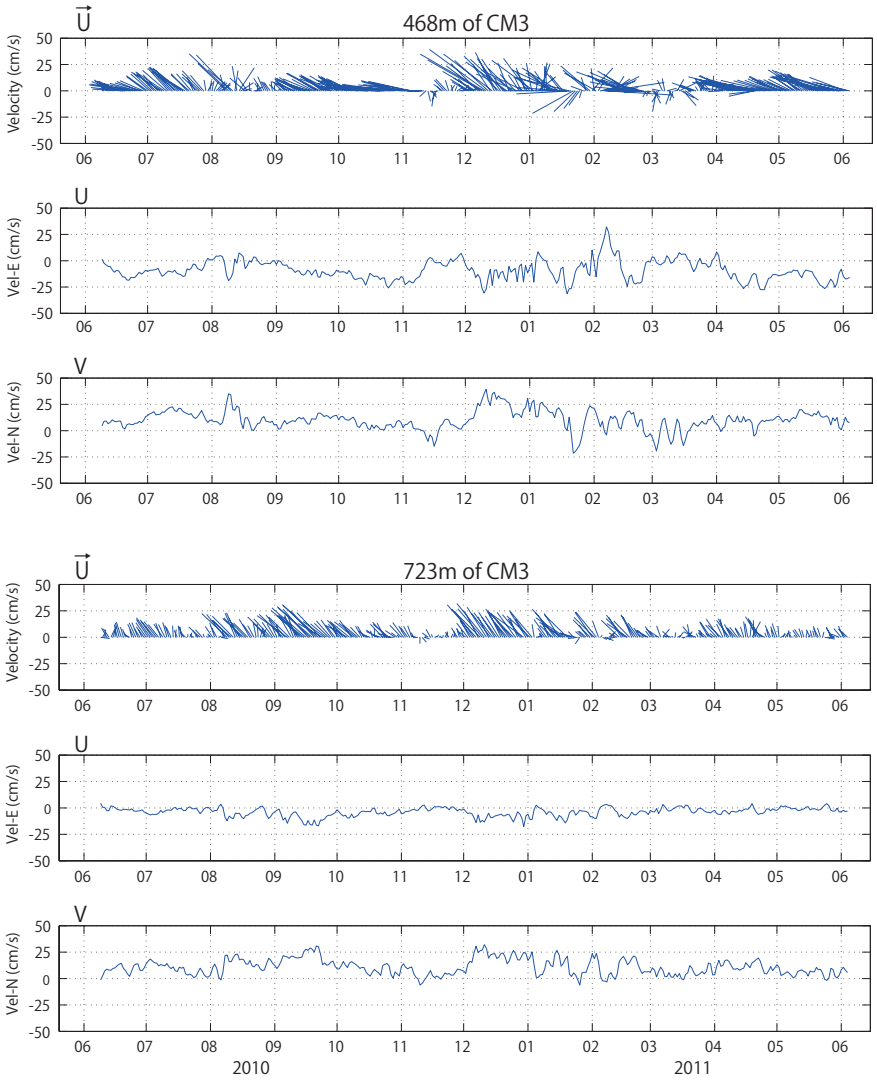

Figure 3.1.2.6. Time series of 3D-ACM current velocities at CM3 for Year 2 (June 2010 – June 2011).

Table. 3.1.2.1. Basic statistics for 3D-ACM current measurements for U (toward True east) and V (toward True north) components (50-hours lowpass filtered). Max and Min denote maximum and minimum values of current components. Direction of vector mean current (50-hours lowpass filtered) is measured clockwise from True north.

ACM	*Year*	Depth (m)	Vel.	Mean cm/s	STD cm/s	Max cm/s	Min cm/s	Vector Mean		Data returned (%)
								Dir (°)	Speed (cm/s)	
CM1 Top	1	443	*U*	-1.76	3.80	8.46	-14.80	342.4	5.84	100
			V	5.56	13.57	52.46	-34.31			
	2	443	*U*	-3.07	5.89	28.14	-12.92	331.0	6.33	100
			V	5.53	11.85	41.24	-28.12			

CM1 Bottom	1	698	*U*	0.62	1.40	3.83	-3.36	120.9	0.72	100
			V	-0.37	6.08	16.89	-20.20			
	2	698	*U*	-0.10	2.49	7.11	-6.25	181.6	3.47	
			V	3.47	7.96	27.10	-18.63			
CM2 Top	1	365	*U*	0.01	7.92	17.10	-24.67	0.1	10.15	100*1)
			V	10.15	14.02	50.34	-21.33			
	2	548	*U*	-3.98	6.80	21.19	-16.65	337.4	10.35	
			V	9.56	10.83	38.51	-22.07			
CM2 Middle	1	620	*U*	0.35	6.20	21.64	-16.33	2.7	7.35	100
			V	7.33	11.13	29.82	-18.85			
	2	753	*U*	-1.25	3.10	9.06	-11.19	348.6	6.33	
			V	6.20	7.99	32.02	-11.23			
CM2 Bottom	1	975	*U*	0.17	3.89	13.24	-10.14	3.8	2.50	100
			V	2.49	5.49	17.49	-14.11			
	2	1008	*U*	2.01	2.79	8.28	-7.94	56.2	2.42	
			V	1.35	3.64	12.74	-7.88			
CM3 Top	1	470	*U*	-1.96	6.91	16.06	-27.67	348.7	10.01	100
			V	9.82	10.19	44.06	-19.12			
	2	468	*U*	-9.17	9.41	32.16	-31.31	317.5	13.58	
			V	10.01	9.34	39.28	-21.41			
CM3 Bottom	1	725	*U*	-0.87	3.99	8.64	-13.88	355.8	11.96	100
			V	11.92	10.56	40.21	-7.59			
	2	723	*U*	-3.94	4.16	4.40	-17.67	340.0	11.55	
			V	10.86	7.60	32.02	-6.23			

*1) The data record was available only until 8 February 2010 for Year 1 because the current meter was severed from the mooring and drifted on the sea surface; but it was fortunately recovered by Japanese fishermen.

3.2 *CPIES*

3.2.1 Pressure (*P*)

Sensor drifts for the CPIES instruments at sites ES1, ES2 (Year 2) and ES3 (Year 2) were determined from their pressure records by first removing obvious "jumps" and "spikes," as well as tides using the response method [*Munk and Cartwright*, 1966], and then fitting coefficients *A, B, C, D* in the equation

$$Drift = Ae^{Bt} + Ct + D \qquad (1)$$

to each record, beginning at a time (t_0) at which the pressure sensor had stabilized (about 12 hours after deployment). In each case, the drift was subtracted from the record. Table 3.1.2.1 gives the values obtained for the drift coefficients. Figure 3.2.1.1 shows the form of these drifts.

Table 3.2.1.1. Values for CPIES pressure sensor drift coefficients in Equation (1) *with time* (t) *in days after* t_0 *(about 12 hours after the deployment). Note: yearday is in days since 2009 January 1, 0 GMT.*

Instrument	$A\times10$	$B\times10^2$	$C\times10^4$	D	t_0 (yearday)
ES1	–1.7392	–5.2397	4.1665	587.355	157.0531
ES2 (Year2)	–1.2754	–6.6123	0.9208	1100.885	525.3875
ES3 (Year2)	–2.7756	–4.6397	8.7538	1037.469	525.3474

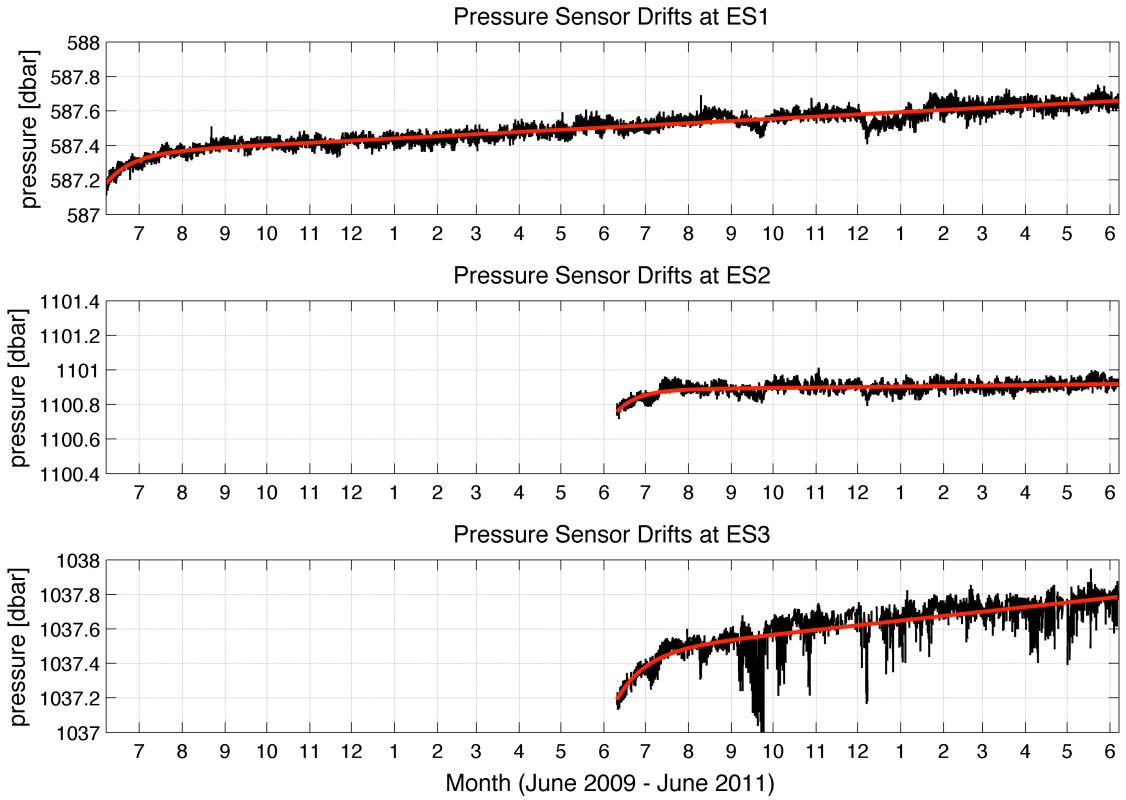

Figure 3.2.1.1. Pressure records (black) and sensor drifts (red) given by the coefficients in Table 3.1.2.1, for the CPIESs at ES1, ES2 (Year 2) and ES3 (Year2), upper, middle and lower panels respectively. Time axis tick marks correspond to beginnings of designated months.

Other pressure records show so much activity that the drift could not be reliably estimated. Strong signals in many of the pressure records at times of strong currents

(speeds up to 60 cm/s) suggest that these CPIES instruments were dragged by the currents along the sea bed, with resulting changes in orientation and depth (see Figures 3.2.4.3-3.2.4.5). As a result, the pressure records were mainly useful only in enabling us to correct the acoustic-travel-time records for these depth changes (see Section 3.2.3 below). Typical vertical temperature gradients at ES1 and ES4 are $0.035°C\ m^{-1}$, so the depth changes would have resulted in temperature changes of only a few hundredths of a degree; we have not made any corrections to the CPIES temperature time series.

3.2.2 Temperature (*T*)

Temperature was measured both in the main CPIES housing (about 1 m above the sea bed) and within the current sensor (about 50 m above the sea bed). Since the Digiquartz sensor is in the interior of the CPIES, its temperature measurement lags the surrounding water temperature by about 2–3 hours. Time series of these temperature records are shown in Figures 3.2.4.1 (ES1), 3.2.4.2 (ES4), 3.2.4.3 (ES2), 3.2.4.4 (ES3) and 3.2.4.5 (ES5).

3.2.3 Acoustic Travel Time (τ)

As described in Section 2.1 above, the CPIES instruments recorded 24 acoustic travel times each hour. These were converted to a single hourly acoustic-travel-time measurement using the quartile method (see *Kennelly et al.*, 2007, Section 3.5.1).

The hourly acoustic-travel-time records from ES1 and ES4 were modified using the pressure records to remove the effects of these changes in instrument depth. In the pressure records, we assumed components from pressure-sensor drift (in ES4) and geostrophic pressure changes (in both ES1 and ES4) were negligible compared with the depth-change signals. In each case, the pressure was first converted to depth (assuming $\rho = 1030\ kg\ m^{-3}$, $g = 9.81\ m\ s^{-2}$) and the corresponding changes in the acoustic travel time were calculated using average sound speed for the depth, temperature and salinity for the CPIES location (temperature and salinity being determined from the mean, for the nominal CPIES depth, of the hydrocast data at the sites shown in Fig. 13). The acoustic-travel-time records were then corrected for these depth changes.

3.2.4 Lowpass filtering and decimation of *P*, *T* and τ records

The resulting records were despiked, then lowpass filtered using a 4^{th} order Butterworth filter passed forward and backward, with cutoff period of 72 hours (3 days). To minimize effects of start up transients, 1 day at the beginning and 1 day at the end of the filtered records were excised. Finally the lowpass-filtered data were subsampled at 12 hour intervals. Time series of these processed *P*, *T* and τ data are plotted in Figures

3.2.4.1 and 3.2.4.2. Time series from ES2, ES3, and ES5 are also plotted in Figures 3.2.4.3, 3.2.4.4, and 3.2.4.5.

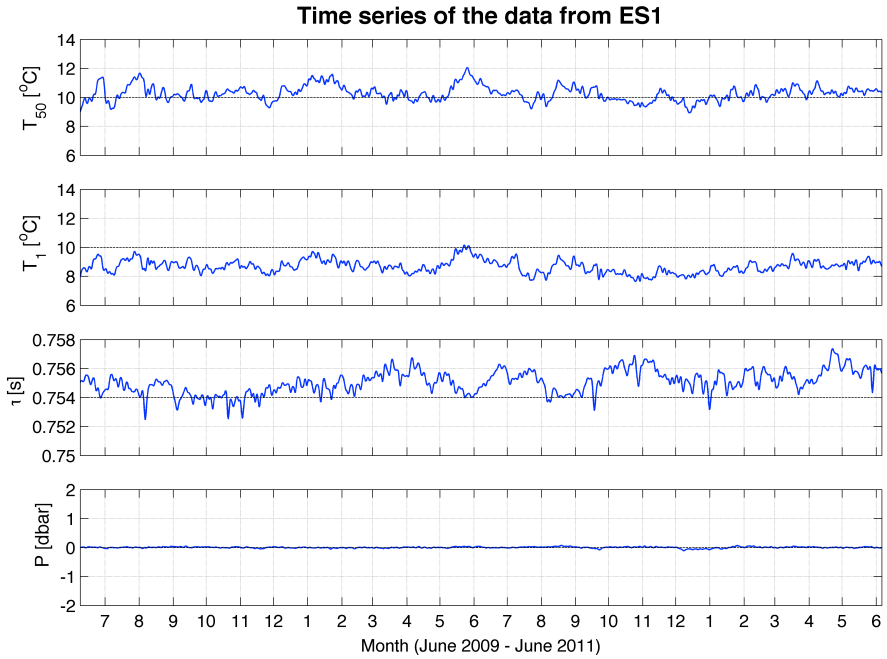

Figure 3.2.4.1. Time series of processed data from the ES1 CPIES instrument. From top: temperature 50 m above bottom T_{50}, temperature 1 m above bottom, T_1, acoustic-travel-time τ, and pressure P (mean removed). Time axis tick marks correspond to beginnings of designated months.

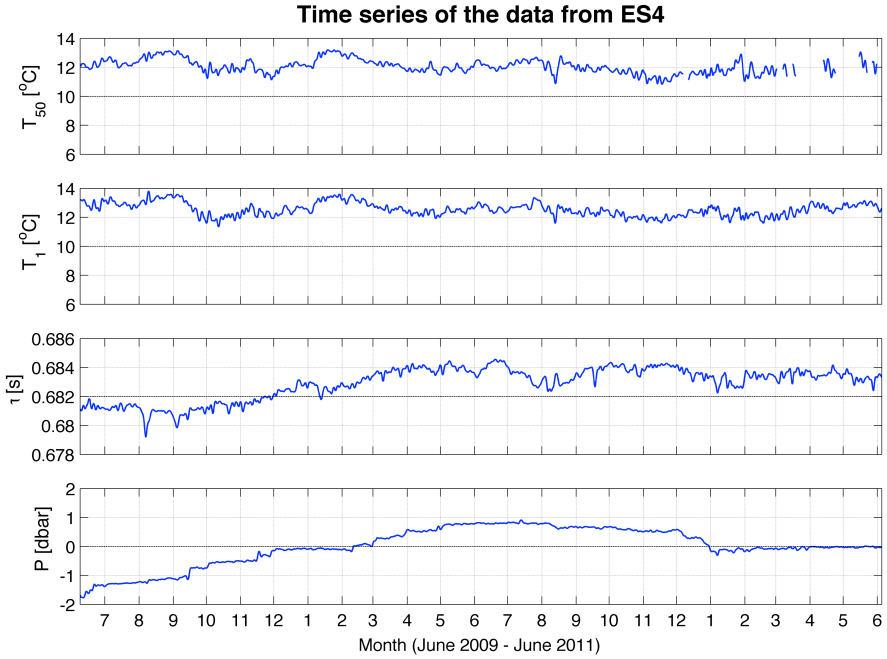

Figure 3.2.4.2. Same as Figure 3.2.4.1 but for the ES4 CPIES instrument. Note that y-axis ranges are the same as those in Figure 3.2.4.1.

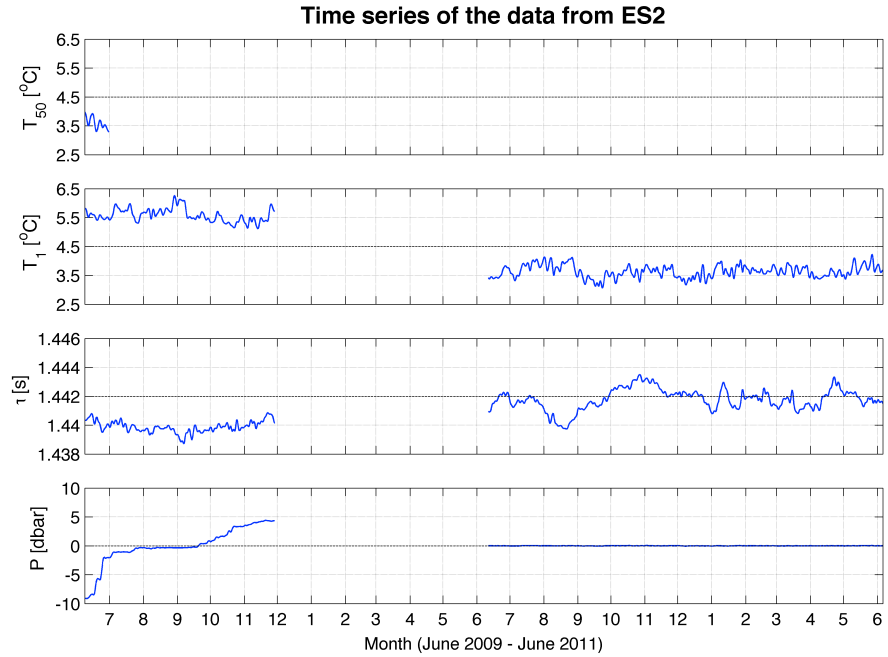

Figure 3.2.4.3. Same as Figure 3.2.4.1 but for the ES2 CPIES instrument. Time axis tick marks correspond to beginnings of designated months.

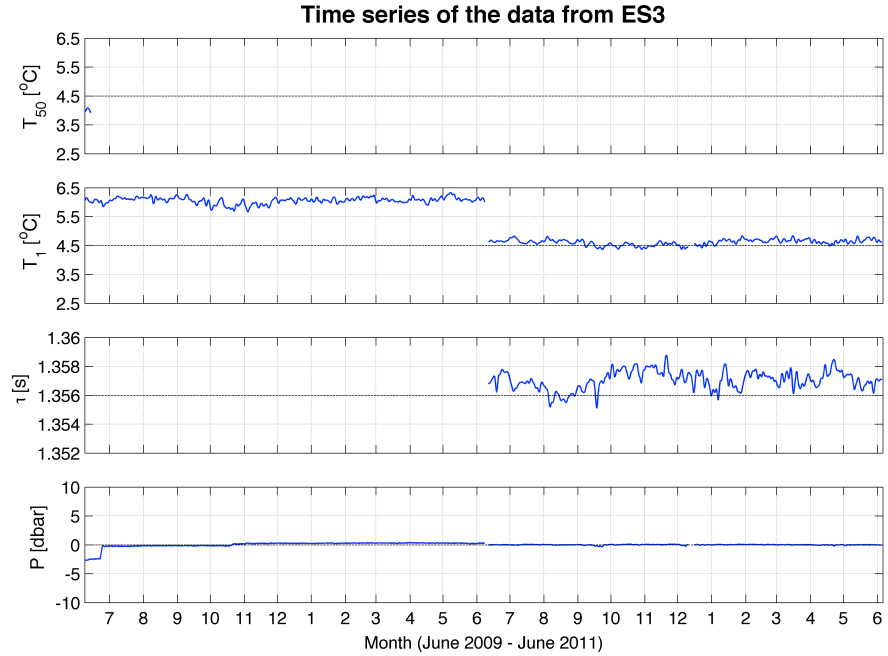

Figure 3.2.4.4. Same as Figure 3.2.4.1 but for the ES3 CPIES instrument. Note that y-axis ranges are the same as those in Figures 3.2.4.3 and 3.2.4.5.

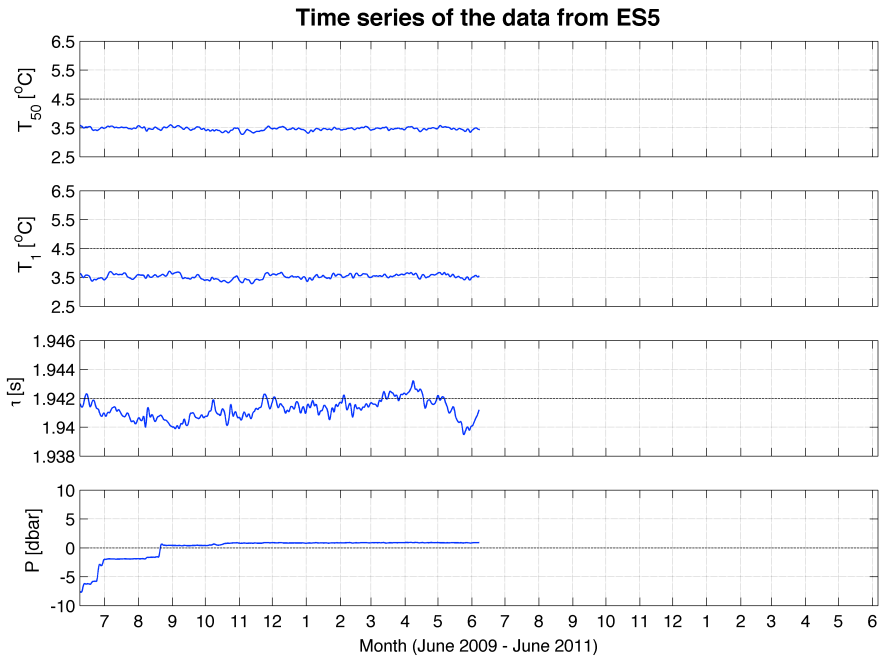

Figure 3.2.4.5. Same as Figure 3.2.4.1 but for the ES5 CPIES instrument. Note that y-axis ranges are the same as those in Figures 3.2.4.3 and 3.2.4.4.

3.2.5 Current Velocity ($\vec{U}$)

Current records at ES1, ES4 and ES5 were corrected (using a routine from NOAA's National Geophysical Data Center, see http://www.ngdc.noaa.gov/geomagmodels/) for the local magnetic declination at each time and at each site (see Table 3.2.5.1 for mean values), so U is true eastward and V is true northward. The velocities were then lowpass filtered using a 4th order Butterworth filter, run forward and backward, with cutoff period of 72 hours (i.e., 3 days). The resulting records were truncated by 1 day at the beginning and 1 day at the end of the filtered records, to minimize effects of start up transients, and subsampled at 12-hour intervals. The results are shown in Figures 3.2.5.1, 3.2.5.2, 3.2.5.3 and 3.2.5.4. Table 3.2.5.2 gives basic statistics for the currents at the two sites; note that the maximum speeds shown in the second-to-last column of this table suggest tidal currents of 40-60 cm/s, since these would be eliminated by the lowpass filtering.

Table 3.2.5.1. Mean magnetic declination at CPIES and CM sites for the deployment time period.

Site	ES1	ES4	ES5	CM1	CM2	CM3
°W	4.4193	4.5079	4.4529	4.4373	4.4647	4.4920

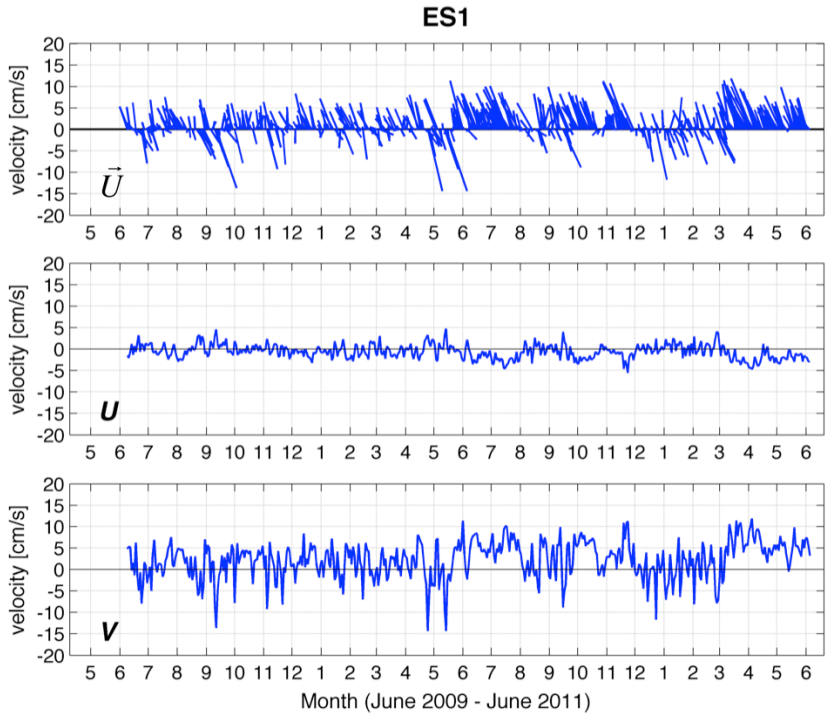

Figure 3.2.5.1. Time series of processed and corrected current data from the ES1 CPIES instrument. From top: current velocity $\vec{U}$, current component U and V. Vertical axis is toward True north. Time axis tick marks correspond to beginnings of designated months.

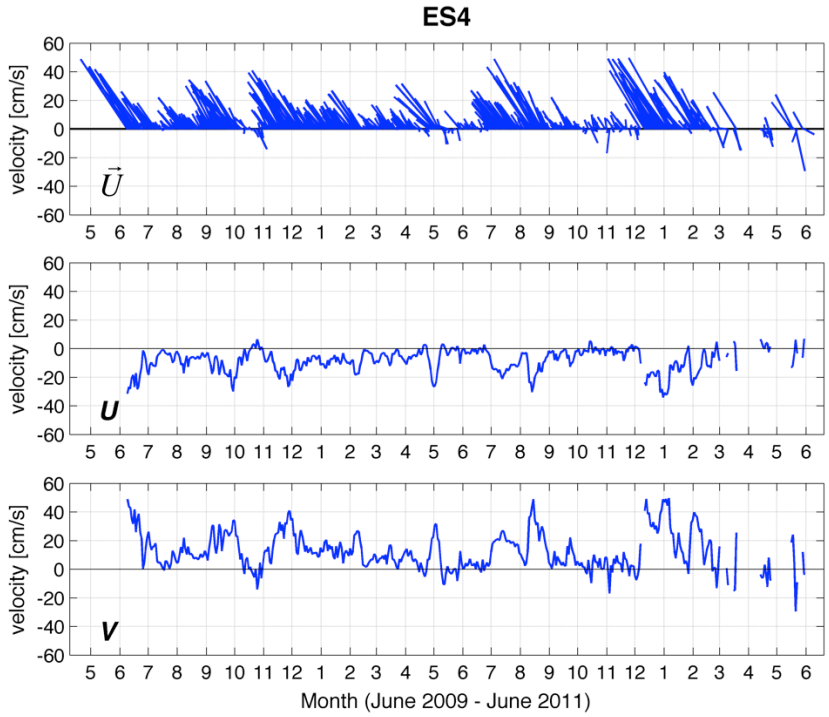

Figure 3.2.5.2. Same as Figure 3.2.5.1 but for the ES4 CPIES instrument. Note that y-axis ranges are different from those in Figure 3.2.5.1.

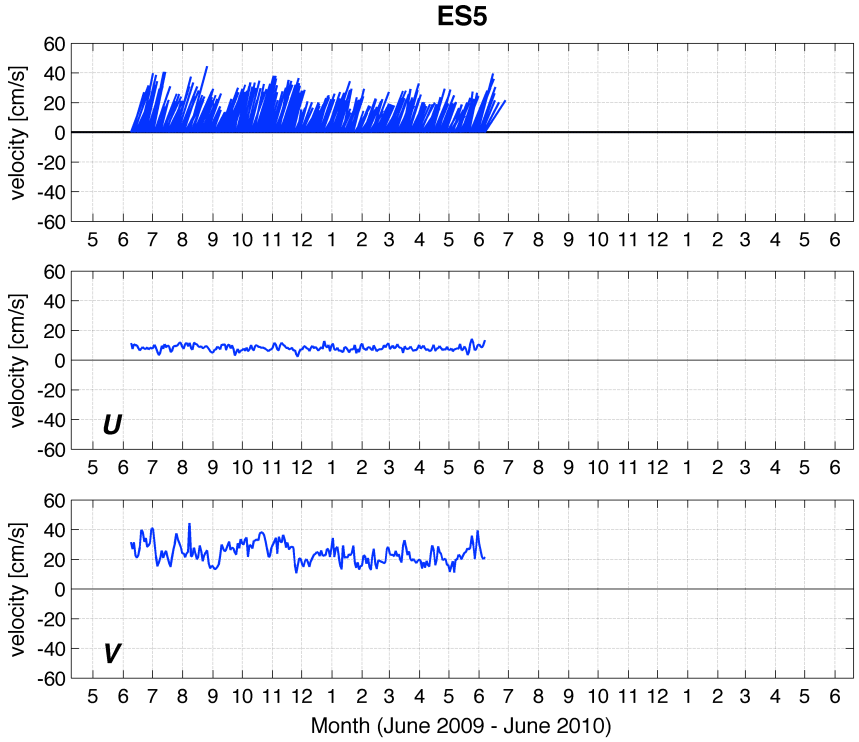

Figure 3.2.5.3. Same as Figure 3.2.5.2 but for the ES5 CPIES instrument.

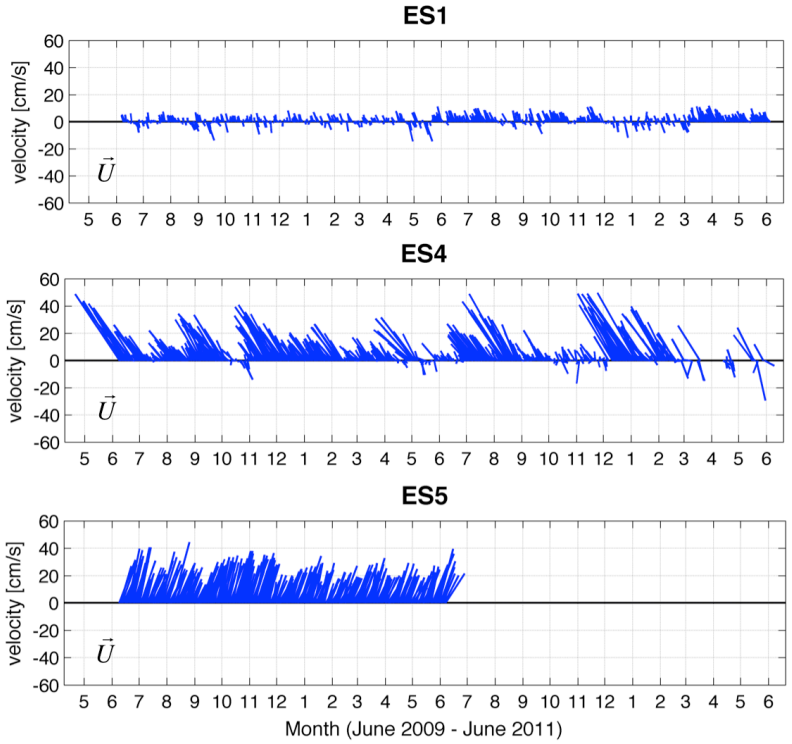

Figure 3.2.5.4. Current velocity $\vec{U}$ from the ES1 (top), ES4 (middle) and ES5 (bottom) CPIES instruments plotted on the same scale. Vertical axis is toward True north. Time axis tick marks correspond to beginnings of designated months.

Table 3.2.5.2. Basic statistics for CPIES current measurements 50 m above bottom for U (toward True east) and V (toward True north) components (72-hour lowpass filtered). Max and Min denote maximum and minimum values of current components. Vector mean current direction is measured clockwise from True north. Maximum Speed values represent maximum lowpass-filtered speed (top) and non-lowpass-filtered speed (bottom, in parentheses).

CPIES	Year	Depth (m)	Vel.	Mean (cm/s)	STD (cm/s)	Max (cm/s)	Min (cm/s)	Vector Mean		Max Speed (cm/s)	Data returned (%)
								Dir (°)	Speed (cm/s)		
ES1	1&2	514	*U*	-0.67	1.68	5.21	-5.57	342.6	2.25	16.10 (69.86)	100
			V	2.14	4.33	12.04	-15.31				
	1		*U*	-0.22	1.47	5.21	-3.71	348.0	1.07	16.10 (67.25)	100
			V	1.04	4.02	11.32	-15.31				
	2		*U*	-1.13	1.75	4.01	-5.57	340.9	3.44	13.23 (69.86)	100
			V	3.25	4.35	12.04	-12.81				
ES4	1&2	456	*U*	-8.39	7.96	9.05	-34.84	325.8	14.92	59.71 (90.92)	91.2
			V	12.34	12.95	50.54	-29.38				
	1		*U*	-8.72	7.22	7.17	-32.16	325.1	15.23	58.12 (87.65)	100
			V	12.49	11.19	48.84	-17.19				
	2		*U*	-7.98	8.77	9.05	-34.84	326.7	14.53	59.71 (90.92)	82.2
			V	12.14	14.87	50.54	-29.38				
ES5	1	1366	*U*	8.13	1.87	14.34	1.89	18.7	25.38	45.95 (83.01)	100
			V	24.04	6.50	44.47	10.58				

4. Shipboard Measurements

4.1 Hydrographic Data

Hydrographic profiles of temperature *T* and salinity *S* were taken near each mooring, as well as other sites, on all three cruises to the KG region. Table 4.1.1 lists the locations, depths and times of these casts. Figure 4.1.1 shows the *T* and *S* sections across the main KG array line for each of the three years.

*Table 4.1.1. Locations, depths and times of CTD and XBT casts during the three KG cruises. Station names with * are those used for the hydrographic sections in Figure 4.1.1. "Distance" is calculated from site KGES1 (southwesternmost station) in each year. XBT station names begin with* "X".

Station name	Latitude (°N)	Longitude (°E)	Distance (km)	Cast depth (m)	Cast time year/mo/day hr GMT
KGES1*	25.6398	126.8222	0	568	2009/06/09 00:10
KGES2*	25.7079	126.9092	11	1083	2009/06/09 03:33
KGES3*	25.8186	127.0316	28	1134	2009/06/09 07:27
KGES4*	25.9139	127.1430	44	506	2009/06/09 10:39
KGES5	25.8328	126.9144		1515	2009/06/08 10:00
KG1	25.5867	126.7578		173	2009/06/08 23:09
KGCM1*	25.6990	126.8647	7	808	2009/06/09 01:24
KGCM2*	25.7798	126.9751	21	1237	2009/06/09 05:20
KGCM3*	25.8543	127.0868	35	817	2009/06/09 09:21
KG2	25.9598	127.1887		87	2009/06/09 11:46
KGES1*	25.6353	126.8316	0	491	2010/06/08 05:50
KGES2*	25.7127	126.9023	11	1064	2010/06/10 06:29
KGES3	25.8074	127.0218		981	2010/06/08 09:48
KGES3-2*	25.8100	127.0253	27	1000	2010/06/10 04:08
KGES4*	25.9122	127.1416	44	520	2010/06/08 12:15
KGES5	25.8218	126.9260		1378	2010/06/09 04:19
XKG1	25.6247	126.8100		436	2010/06/10 08:32
XKG2	25.6699	126.8650		768	2010/06/10 09:00
XKG3	25.7138	126.9200		1180	2010/06/10 09:27
XKG4	25.7641	126.9699		1091	2010/06/10 09:54
XKG5	25.8164	127.0224		1049	2010/06/10 10:22
XKG6	25.8592	127.0749		910	2010/06/10 10:49
XKG7	25.8879	127.1302		626	2010/06/10 11:13
KGES1*	25.6478	126.8323	0	545	2011/06/07 05:18
KGES2*	25.7180	126.9024	10	1085	2011/06/07 03:44
KGES3*	25.8199	127.0293	27	1054	2011/06/06 09:03
KGES4*	25.9163	127.1462	43	481	2011/06/06 06:32
K01	26.3028	126.6519		675	2011/06/07 23:43
K02	26.1440	126.5966		1577	2011/06/08 01:50
K03	25.9808	126.5629		1760	2011/06/08 07:45
K04	25.8980	126.5354		649	2011/06/08 09:34
K05	25.7943	126.5068		512	2011/06/08 10:58
K06	25.8007	126.7697		432	2011/06/08 23:10
K07	25.8986	126.8408		1685	2011/06/09 00:37
K08	25.9939	126.9056		1644	2011/06/09 03:25
K09	26.0815	126.9763		981	2011/06/09 04:48
K10	26.1721	127.0357		660	2011/06/09 06:28

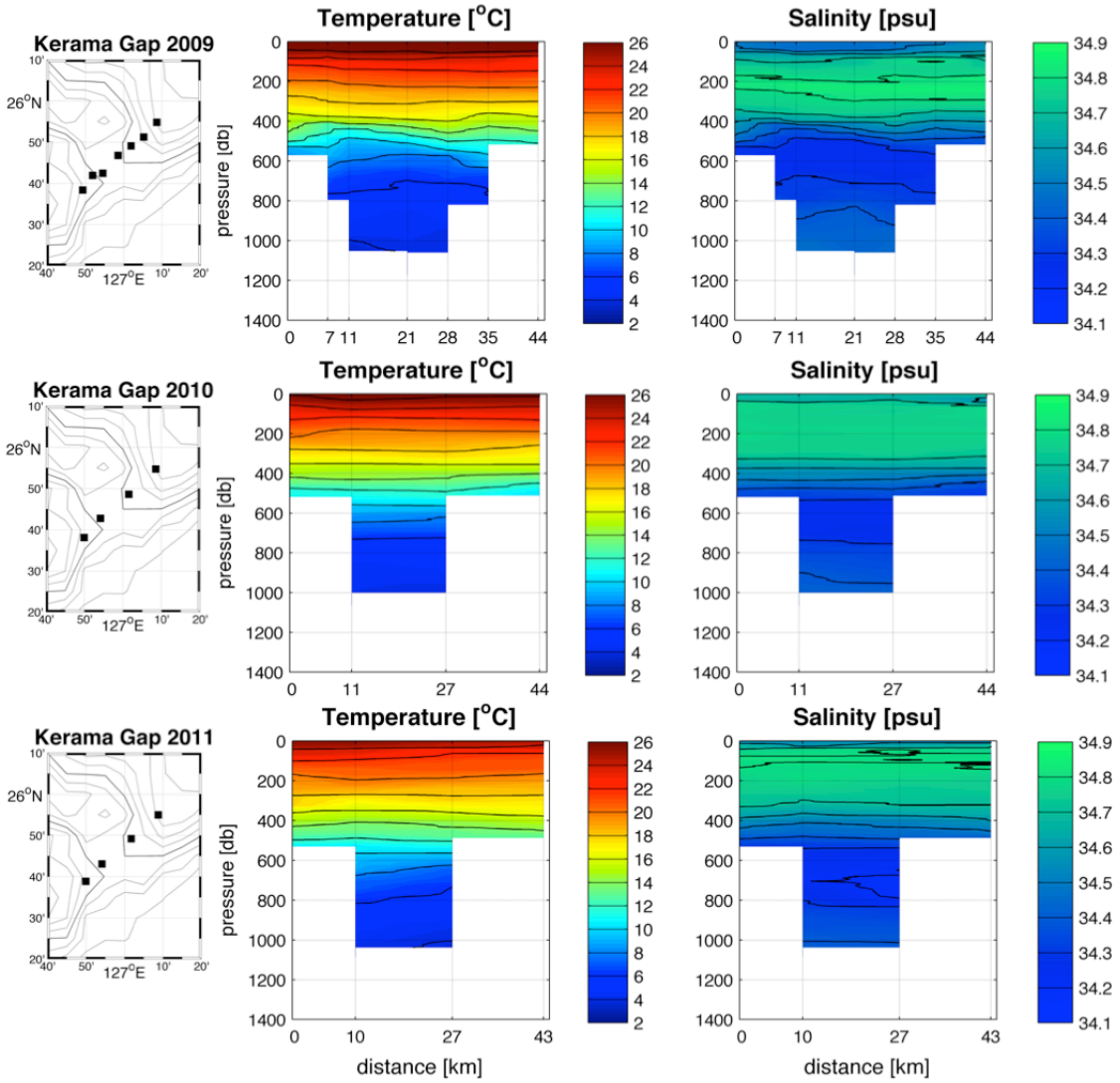

Figure 4.1.1. Hydrographic sections across the main mooring array: station map (left), temperature T (middle), and salinity S (right) for cruises in June 2009 (top), 2010 (middle) and 2011 (bottom). Contour intervals are 2°C (T) and 0.1 psu (S).

4.2 ADCP Data

4.2.1 Methods

Continuous current measurements along lines connecting CPIES and CM mooring stations were carried out using a hull-mounted ADCP (RD Instruments OS-75 system) with the ship's main gyrocompass and the ship's D-GPS navigation system. The firmware version of the ADCP was 23.17 and the data acquisition software was VmDas Ver.1.42. The ADCP was configured for the narrow-band and bottom-tracking modes, recording each ping as raw data for 45 bins with 16 m interval in depths from 31 m to

735 m. Raw data, short-term averaged data (STA: 60 seconds), and long-term averaged data (LTA: 300 seconds) were recorded. Table 4.2.2.1 indicates a list of the ADCP measurements, and Figure 5.1 shows examples of velocity sections for the 2010 and 2011 cruises.

4.2.2 Data Processing

The data obtained by the ADCP were processed using CODAS software Ver. 3.1 with Quick_adcp.py [*Firing et al.*, 1995]. The misalignment angle of the transducer heading was -0.7214 degrees in the 2009 cruise and 0.2909 degrees in the 2010 cruise.

Table 4.2.2.1. Periods, locations and data filenames of ADCP measurements for the 2010 and 2011 cruises.

Period	Position				Data Filename
year/mo/day hr:mm – mo/day hr:mm (UTC)	Start		End		
	Latitude (°N)	Longitude (°E)	Latitude (°N)	Longitude (°E)	
2010/6/7 02:08 – 6/7 20:20	25.9622	127.1993	25.5986	126.7677	KG2010_1*.*
2010/6/8 06:21 – 6/8 11:13	25.6500	126.8224	25.8947	127.1181	KG2010_2*.*
2010/6/9 13:48 – 6/9 17:08	25.5955	127.7674	25.9616	127.1944	KG2010_3*.*
2010/6/9 17:08 – 6/10 08:26	25.9616	127.1944	25.6239	126.8042	KG2010_4*.*
2010/6/10 08:27 – 6/10 11:16	25.6239	126.8042	25.9112	127.1314	KG2010_5*.*
2011/6/7 04:16 – 6/7 04:49	25.7125	126.8937	25.6599	126.8276	KG2011_1*.*
2011/6/6 21:18 – 6/6 22:27	25.8529	127.0823	25.7875	126.9815	KG2011_2*.*

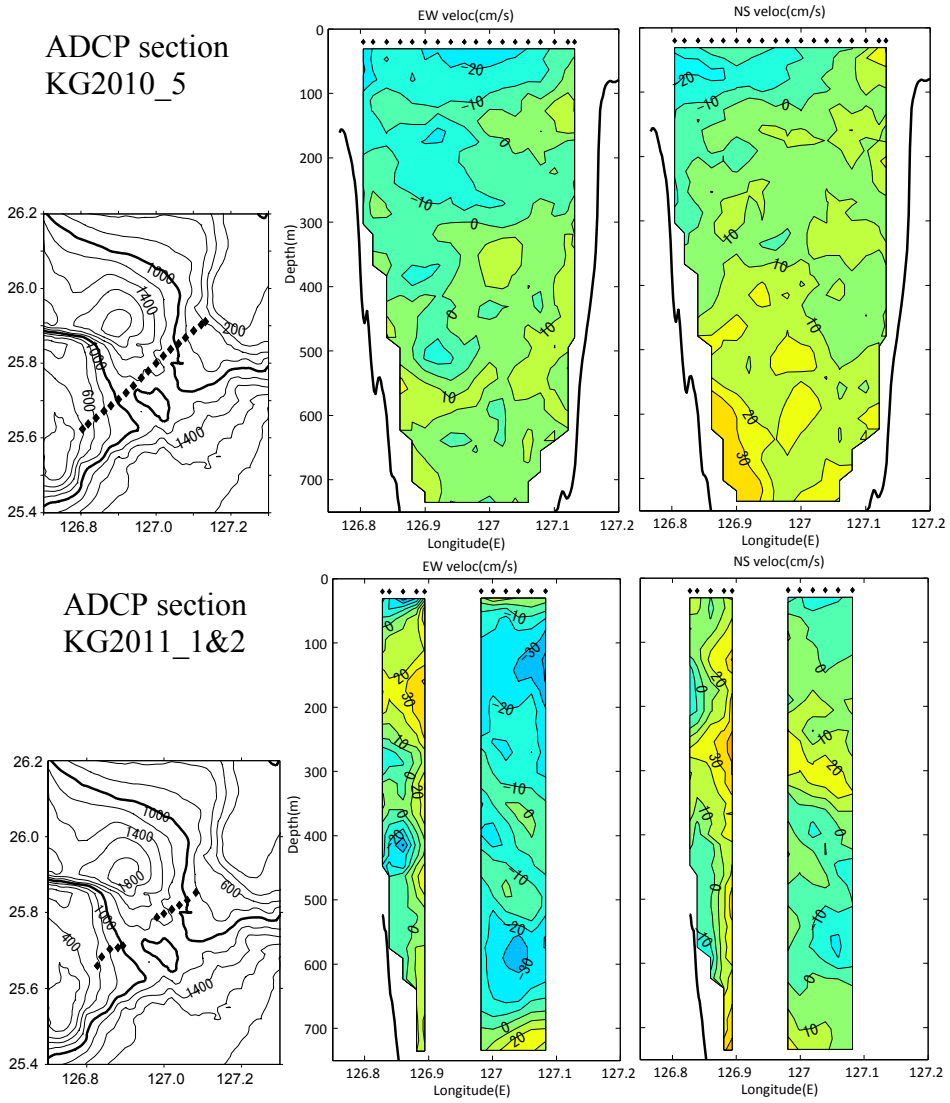

Figure 4.2.2.1. ADCP velocity sections (cm/s) measured on June 10 for the 2010 cruise (upper panels) and on June 6–7 for the 2011 cruise (lower panels) : station map (left), velocity component U (middle), and velocity component V (right).

5. GEMs

The vertical structures of the current and temperature fields are related to vertically integrated quantities such as acoustic travel time τ (e.g., a deeper thermocline is associated with a shorter acoustic travel time). For a given region, this relationship (if it exists), between the vertical profile of temperature (T) or specific-volume-anomaly (δ) and acoustic travel time (τ) can be determined from hydrographic data. The part of the vertical structure that is captured by this relationship is the "Gravest Empirical Mode" (GEM) [*Meinen and Watts, 2000, Book et al.*, 2002].

To compute suitable GEMs, we used 167 hydrographic profiles from the region near the KG (Figure 5.1). These included historic profiles from the World Ocean Atlas (WOA) 2009, the North Pacific Hydrobase [*Macdonald et al.*, 2001] and the Nagasaki Marine Observatory (NMO), Japan Meteorological Agency (duplicates removed), plus Argo float data and the 28 profiles which we obtained on our three cruises (see Section 4.1 above). All of these profiles were quality controlled; they extended to at least 500 dbar. Data were extracted at 10 dbar intervals.

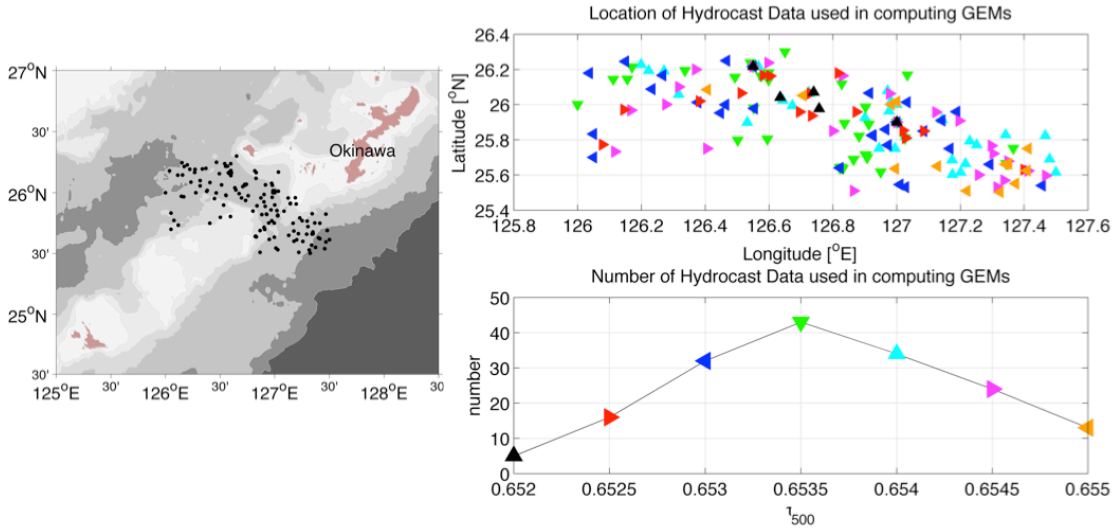

Figure 5.1. Site locations (left and top) and numbers of hydrocasts (bottom) used in computing Gravest Empricial Modes (GEMs) for the Kerama Gap region. Colors in top panel are keyed to corresponding colors in bottom panel.

To compute the GEMs, the hydrographic data were first deseasoned using a method similar to the "Seasonal Model" (SM) method of *Watts et al.* [2001]. For each parameter (T and δ at 10 dbar increments from 0 to 250 dbar), we averaged all the data for a given yearday, thereby producing a one-year record of daily averages (with gaps for those days lacking data). We then replicated this record to form a 3-year time series, to which we applied a smoothing spline (Matlab function **csaps** with smoothing parameter p=0.000025 for T, 0.000001 for δ). To avoid start and end transients, the resulting middle year of the smoothed output was extracted and used as the seasonal signal to be removed in the "deseasoning" procedure. Figure 5.2 shows the SM curves for T and δ at each pressure level from 0 to 150 dbar. Vertical round-trip acoustic travel time from 500 dbar to the surface, τ_{500}, was calculated from the historical hydrographic data using a constant value for gravitational acceleration, g = 9.8 m/s^2 (rather than the local g). This was then deseasoned in the same way (with smoothing parameter p=0.000025). The τ_{500} curve is shown in Figure 5.3. Before computing the GEMs, the hydrographic data were de-seasoned using the seasonal signals shown in Figures 5.2 and 5.3.

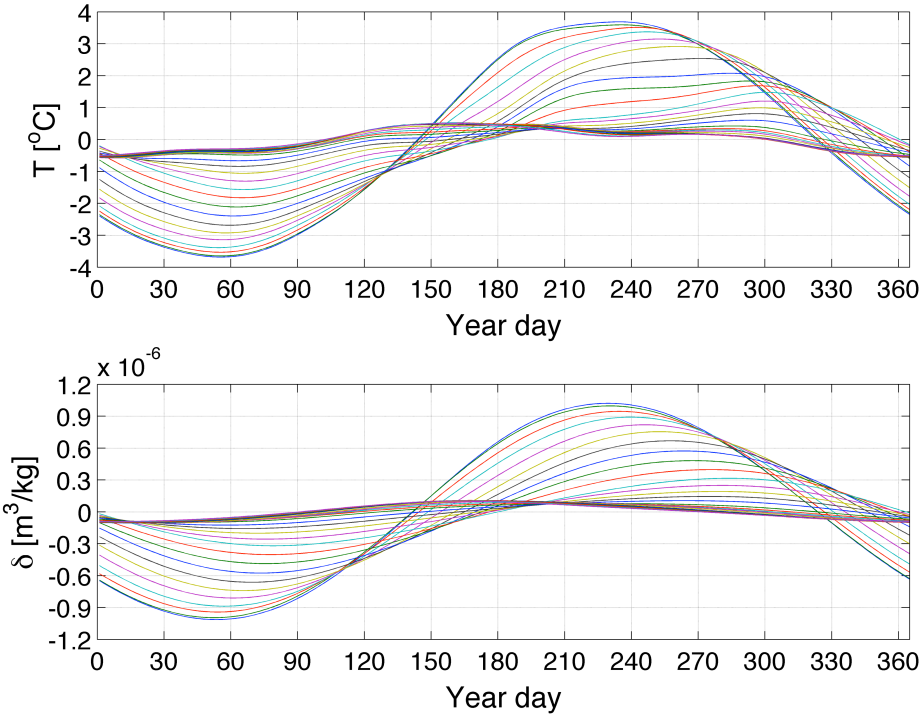

Figure 5.2. SM temperature (top) and specific-volume-anomaly (bottom) seasonal signals, from the surface (largest amplitude) to 150 dbar in 10 dbar increments.

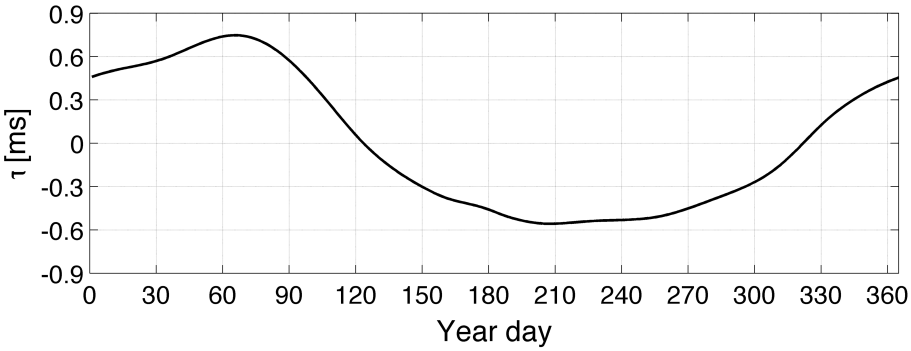

Figure 5.3. SM acoustic-travel-time (τ_{500}) seasonal signal.

Spline fits (Matlab function **csaps** with smoothing parameter p=0 .9999995) were used to quantify the relationship between the deseasoned hydrographic temperature data and deseasoned hydrographic τ_{500} at each pressure level from the surface to 500 dbar in 10 dbar increments. From these, we generated lookup tables of temperature as a function of pressure (in 10 dbar intervals) and τ_{500} (in 0.1 ms intervals). The same procedure was carried out for specific volume anomaly in place of temperature. The resulting temperature and specific-volume-anomaly τ-GEMs computed from the deseasoned data are shown in Figure 5.4.

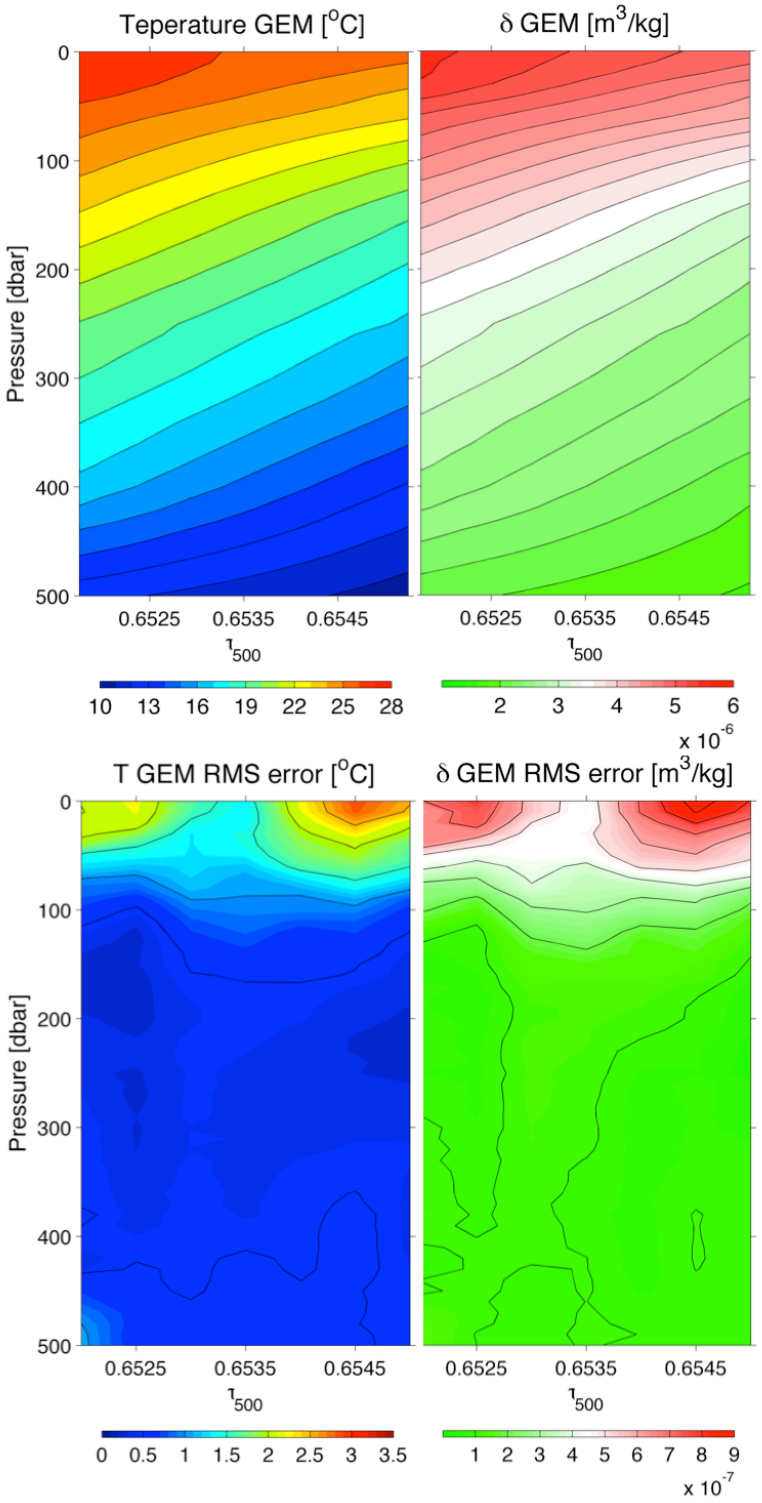

Figure 5.4. Upper panels: Temperature T (left) and specific-volume-anomaly δ (right) GEM fields computed from hydrocasts in the Kerama Gap region. Contours are shown at intervals of 1 °C (left) and 2×10^{-7} m^{-3}/kg (right). These fields allow us to determine T and δ profiles from a measurement of τ_{500}. Lower panels: error fields for corresponding upper panels. Contours are shown at intervals of 0.5 °C (left) and 1×10^{-7} m^{-3}/kg (right).

In order to evaluate how well the τ-GEM represents the vertical structure of the water column, the GEM-predicted temperature and specific-volume-anomaly profiles were compared to the actual temperature and specific-volume-anomaly profiles of the hydrographic data. For each hydrocast, τ_{500} was calculated from the data. Then this was used to look up the GEM-predicted temperature and specific-volume-anomaly profiles. The rms error between the GEM-predicted and hydrocast values was calculated. Then average rms error in 0.5 ms by 10 dbar bins was calculated and contoured as a function of pressure and τ_{500}. These error fields are shown in the lower panels of Figure 5.4. It's important to recognize that actual errors in our 50-hour lowpass filtered transport time series are less than these fields would imply, because shorter-period fluctuations, such as those from second-mode internal tides, probably contribute much to these error fields.

In order to use a GEM lookup table based on τ referenced to 500 dbar, the measured acoustic travel time data from each CPIES instrument must be converted from travel time referenced to the instrument's pressure level, τ_p, to travel time referenced to 500 dbar, τ_{500}. First the pressure level of each instrument is determined from the mean of its dedrifted pressure record minus atmospheric pressure (10.1325 dbar = 1 atm). Then hydrographic data are used to calculate τ_{500} and τ_p for each hydrographic profile extending to this pressure level. These are plotted one against the other in Figure 5.5. Also shown in this figure are least-squares fitted straight lines. Table 5.1 gives the coefficients for these fitted functions.

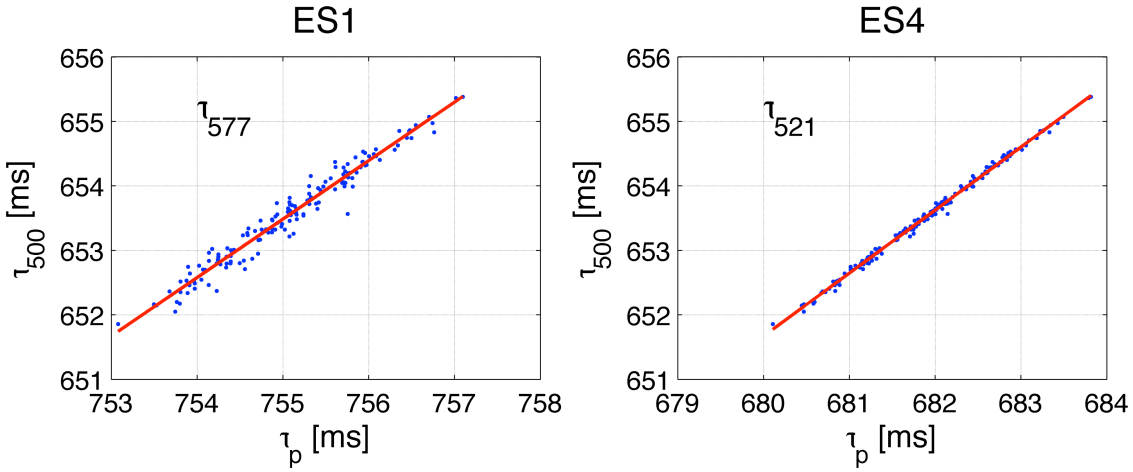

Figure 5.5. τ_{500} plotted with τ_p for CPIESs at ES1 (left) and ES2 (right). Red lines are best-fit straight lines (see Table 5.1).

Table 5.1. Coefficients for the conversion: $\tau_{500} = a_0 + a_1\tau_p$ (τ in ms), representing the red lines in Figure 5.5.

CPIES	a_0	a_1	rms error (ms)
ES1	-31.45	0.91	0.15
ES4	-13.20	0.98	0.05

Acknowledgements

We are grateful for the support and assistance of Captain Masataka Higashi and his crew aboard the T/V Kagoshima-maru. Erran Sousa skilfully prepared the CPIES instruments and directed their deployments and recoveries. Dr. Magdalena Andres assisted with at-sea operations, and Maureen Kennelly helped with data management. Dr. D. Randolph Watts gave frequent valuable advice.

Some of the CTD data used in the GEM calculations were kindly provided by the Nagasaki Marine Observatory, Japan Meteorological Agency. The University of Rhode Island group was supported by ONR Grant number N00014-09-1-0391.

References

Book, J., M. Wimbush, S. Imawaki, H. Ichikawa, H. Uchida, and H. Kinoshita (2002), Kuroshio temporal and spatial variations south of Japan determined from inverted echo sounder measurements, *J. Geophys. Res.*, *107*(C9):3121, (doi:10.1029/2001JC000795)

Choi, B. H., K. O. Kim and H. M. Eum (2002), Digital bathymetric and topographic data for neighboring seas of Korea, *J. Korean Soc. Coastal and Ocean Engrs.*, *14(1)*, 41-50 (in Korean).

Firing E., J. Ranada, and P. Caldwell (1995), Processing ADCP data with the CODAS Software System Version 3.1.
http://currents.soest.hawaii.edu/docs/doc/index.html

Kennelly, M., K. Tracey and D. R. Watts (2007), Inverted echo sounder data processing manual, University of Rhode Island, Graduate School of Oceanography, Narragansett, RI, GSO Technical Report No. 2007-02, 87 pp.

Macdonald, A. M., T. Suga, and R. G. Curry (2001), An isopycnally averaged North Pacific climatology, *J. Atmos. Oceanic Technol.*, *18*, 394–420.

Meinen, C.S., and D.R, Watts (2000), Vertical structure and transport on a transect across the North atlantic current near 42°N: time series and mean, *J. Geophys. Res.*, *105*, 21,869–21,891.

Munk, W. H. and D. E. Cartwright,(1966), Tidal spectroscopy and prediction, *Phil. Trans. R. Soc. London*, *A, 259*, 533-581.

Watts, D. R., C. Sun and S. Rintoul (2001), A two-dimensional Gravest Empirical Mode determined from hydrographic observations in the Subantarctic Front, *J. Phys. Oceanogr.*, *31*, 2186–2209.